




ORIGINAL RESEARCH

# Impaired Elastic Properties of the Ascending Aorta in Fetuses With Coarctation of the Aorta

Ran Xu , MD; Dan Zhou, BD; Yushan Liu, BD; Longmei Yao , BD; Li Xie, BD; Minghui Liu, MD; Qichang Zhou, MD; Shi Zeng , MD

**BACKGROUND:** Abnormal aortic elastic properties are major notable vasculopathy involved in coarctation of the aorta (CoA). However, there are no reports on aortic wall elastic characteristics in fetuses with CoA.

**METHODS AND RESULTS:** Fifty-six fetuses with CoA and 56 normal controls were included in this prospective case–control study. The dimensions of the cardiac chamber, the size of the aorta, left ventricular myocardial performance indexes, and aortic elastic properties, including the global circumferential strain, fractional area change and mean longitudinal strain, were measured serially in utero. The global circumferential strain, fractional area change, and mean longitudinal strain in fetuses with CoA were smaller than those in the normal group at both the first and last examinations (18.50% versus 37.73% for global circumferential strain, 38.90% versus 57.55% for fractional area change, 6.61% versus 11.81% for mean longitudinal strain at first scan, 16.62% versus 42.05% for global circumferential strain, 36.54% versus 59.7% for fractional area change, 6.2% versus 11.46% for mean longitudinal strain at last scan, all  $P < 0.001$ ). There were negative correlations between aortic elastic properties and left ventricular myocardial performance indexes in fetuses with CoA ( $P < 0.01$ ). Aortic elastic properties were correlated positively with aortic isthmus size in fetuses with CoA ( $P < 0.01$ ).

**CONCLUSIONS:** Aortic strain and the fractional area change were decreased in fetuses with CoA. Impairments of these aortic elastic properties were associated with diminished heart function and aortic isthmus size in utero. Further large-scale longitudinal studies are required to confirm the potential predictive value of cardiovascular morbidity (ie, hypertension) in fetuses with CoA.

**Key Words:** coarctation of the aorta ■ elastic properties ■ speckle-tracking;VVI ■ strain

Coarctation of the aorta (CoA) is the fifth most common congenital heart defect and accounts for ≈7% of all congenital heart defects.<sup>1,2</sup> While CoA was originally described as a discrete narrowing in the aortic isthmus, it is considered a general aortopathy involving various segments of the arch. Abnormal elastic properties seem to constitute a major notable aortopathy.<sup>2–4</sup> The importance of impaired vascular properties relies on the fact that patients with CoA have a lifelong risk of cardiovascular morbidity,<sup>5</sup> such as hypertension, coronary heart

disease, heart failure, and sudden death, even in the setting of successful repair. Vogt et al<sup>6</sup> observed reduced aortic distensibility and a higher aortic stiffness index in neonates with CoA preoperatively. Biopsy in neonates with CoA also showed widespread elastic fiber fragmentation in the paracoarctation aortic wall.<sup>7</sup> These limited data suggested that aortic elastic properties may be impaired in the early stages of life. However, it is not clear whether impairments of vascular properties occur primarily during the earliest development period, such as in utero.

Correspondence to: Shi Zeng, MD, Department of Ultrasound, Second Xiangya Hospital of Central South University, 139 Renmin Rd (M), Changsha 410011, China. Email: [shizeng@csu.edu.cn](mailto:shizeng@csu.edu.cn), [doctorzshi@163.com](mailto:doctorzshi@163.com)

Supplemental Material is available at <https://www.ahajournals.org/doi/suppl/10.1161/JAHA.122.028015>

For Sources of Funding and Disclosures, see page 9.

© 2023 The Authors. Published on behalf of the American Heart Association, Inc., by Wiley. This is an open access article under the terms of the [Creative Commons Attribution-NonCommercial-NoDerivs](https://creativecommons.org/licenses/by-nc-nd/4.0/) License, which permits use and distribution in any medium, provided the original work is properly cited, the use is non-commercial and no modifications or adaptations are made.

JAHA is available at: [www.ahajournals.org/journal/jaha](http://www.ahajournals.org/journal/jaha)

## CLINICAL PERSPECTIVE

### What Is New?

- Aortic strain and the fractional area change were decreased in fetuses with coarctation of the aorta.
- Impairments of these aortic elastic properties were associated with diminished heart function and aortic isthmus size in utero.

### What Are the Clinical Implications?

- Impaired elastic properties have potential predictive value of cardiovascular morbidity (ie, hypertension) in fetuses with coarctation of the aorta.

## Nonstandard Abbreviations and Acronyms

<b>AA</b>	ascending aorta
<b>AV</b>	aortic valve
<b>CoA</b>	coarctation of the aorta
<b>FAC</b>	fractional area change
<b>GA</b>	gestational age
<b>GCS</b>	global circumferential strain
<b>MLS</b>	mean longitudinal strain
<b>MPI-LV</b>	left ventricular myocardial performance indexes
<b>VVI</b>	velocity vector imaging

Velocity vector imaging (VVI), a 2-dimensional speckle-tracking technique, was originally proposed as a quantitative tool for assessing cardiac deformation based on the combination of natural ultrasound speckle reflector tracking with complex geometric analysis.<sup>8</sup> VVI has been used to assess fetal cardiac deformation in various conditions by our team, including fetal CoA,<sup>9</sup> fetal lower urinary tract obstruction,<sup>10</sup> and fetal cardiac aneurysms/diverticula.<sup>11</sup> Kim et al first applied this technique to the measurement of aortic mechanics, such as area change and aortic wall strain, and showed a strong correlation with pulse wave velocities, which were the recommended gold standard measurement of arterial stiffness.<sup>12</sup> Recently, VVI has been described as a feasible tool for evaluating aortic elastic function in patients with Turner syndrome<sup>13</sup> and aortic valve diseases.<sup>14</sup> However, there are no reports on fetal aortic wall elastic characteristics by VVI.

The aims of this study were to evaluate the elastic properties of the ascending aorta and longitudinally observe the progress of aortic wall mechanics in fetuses with CoA. The primary outcome of the study was to identify differences in aortic elastic properties between

fetuses with CoA and normal fetuses. A total of 102 patients (1:1 allocation ratio) were required based on the sample size calculated by setting the effect size  $f$  at 0.5,  $\alpha$  at 0.05, and power at 0.80.

## METHODS

A longitudinal observational study was performed at The Second Xiangya Hospital of Central South University in China from February 2013 to January 2020. The case group consisted of pregnant mothers referred for fetal echocardiography attributable to great artery or ventricular disproportion. The inclusion criteria were fetuses with an aortic isthmus z-score based on gestational age (GA)  $<-2$  in either the sagittal or 3-vessel trachea view accompanying abnormal flow at the aortic isthmus and confirmed by pediatric cardiologists as CoA by postnatal clinical and imaging data. The exclusion criteria were fetuses with hypoplastic left heart syndrome, mitral or tricuspid malformation, abnormal atrioventricular or ventricular-arterial connection, medium or large ( $>2$  mm) ventricular septal defect, and anomalous pulmonary venous return. The GA-matched control normal group comprised fetuses of low-risk pregnant women. Furthermore, we excluded fetuses whose mothers had multiple gestation; those who had a GA  $<18$  weeks; those who were small for their gestational age; those with extracardiac or chromosomal defects; those with persistent fetal arrhythmia; or those whose mothers had maternal complications, including preeclampsia, gestational diabetes, and thyroid disease. Each fetus was serially scanned at 4-week intervals. For the purpose of this study, only information from the first and last examinations was included. Written informed consent was obtained from all the families. This study was approved by the institutional review board at The Second Xiangya Hospital of Central South University. The data that support the findings of this study are available from the corresponding author upon reasonable request.

Routine obstetrical ultrasound and heart examinations were performed using an Acuson Sequoia 512 system (Siemens Medical, WA) with a 6C2 transducer. Fetal biometry, including the biparietal diameter, head circumference, abdominal circumference, and femoral length, was measured and used to calculate the estimated fetal weight. A standard fetal echocardiogram was performed by an expert (QC.Z.). The dimensions of cardiac chambers and valves were measured at their maximal size following the inner-to-inner edge model<sup>15</sup> and were converted automatically to z-scores based on GA. The mitral valve, tricuspid valve, left ventricle (LV), and right ventricle (RV) were obtained in the 4-chamber view in diastole. The aortic valve (AV), ascending aorta (AA), and descending

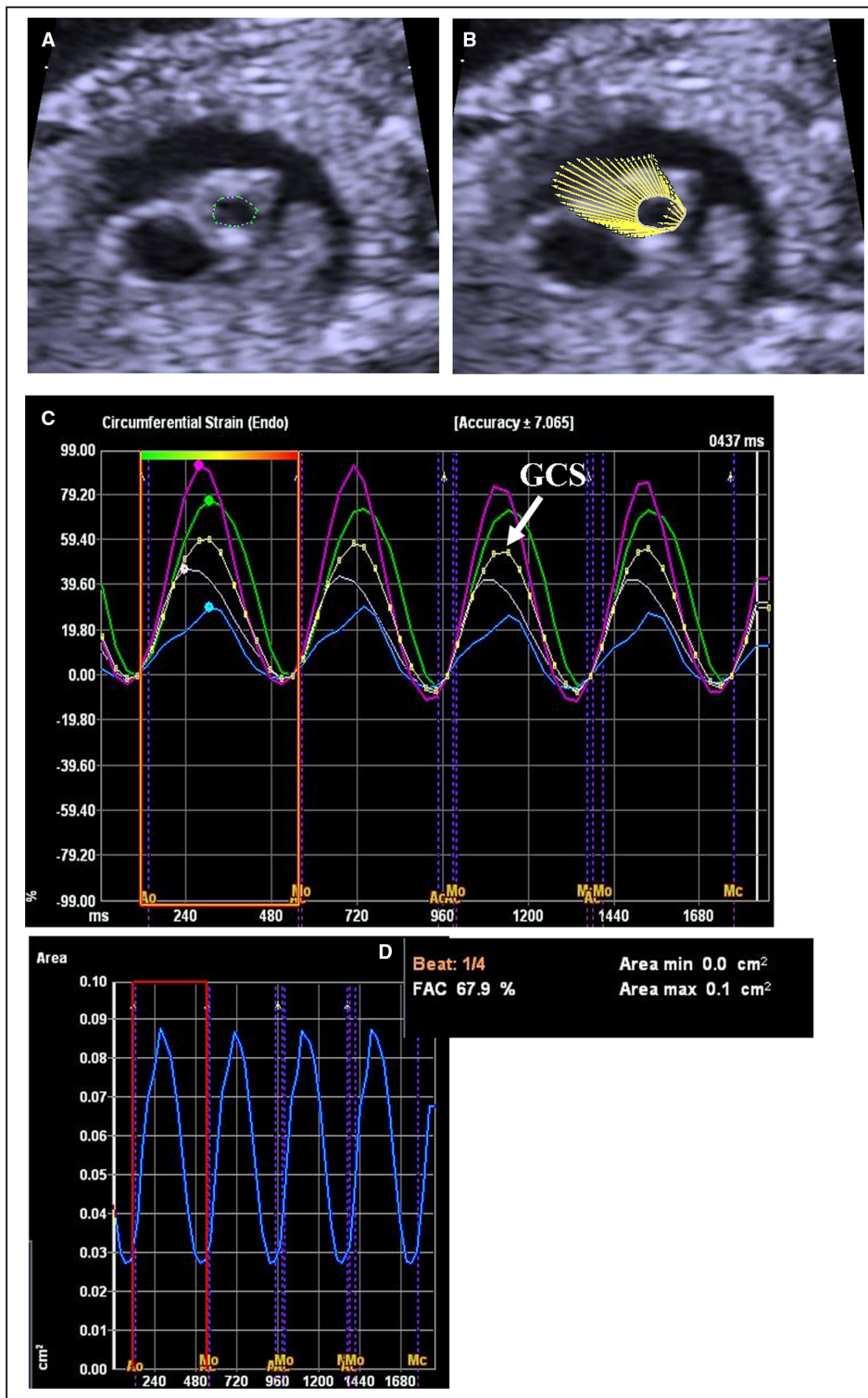


**Figure 1.** Obtainment of the global circumferential strain and fractional area change by the velocity vector imaging technique.

**A**, Tracing along ascending aorta border in a still frame of the ascending aorta with optimal blood-intima border visualization in short-axis view. **B**, The velocity vector image of traced ascending aorta. **C**, Circumferential strain during cardiac cycle were automatically calculated and displayed in a segment model with different colors. The global circumferential strain (indexed by white arrow) was calculated as the average of all segmental circumferential strains and thus represented ascending aorta wall circumferential deformations. **D**, The cross-sectional area curve of the aortic lumen during the heart cycle is displayed. The fractional area change was calculated automatically as the percent change in the cross-sectional area: fractional area change (%)=(largest cross-sectional area -smallest cross-sectional area)/(largest cross-sectional area)×100. GCS indicates global circumferential strain.

aorta were obtained in longitudinal view in systole. The aortic isthmus size was measured in both sagittal and 3-vessel trachea views. The modified left ventricular myocardial performance indexes (MPI-LV) were obtained in the 5-chamber view and calculated using pulse Doppler methods<sup>16</sup>: MPI-LV is defined as the sum of isovolumetric contraction time (ICT) and isovolumetric relaxation time (IRT) divided by ejection time (ET), where ICT refers to the interval time from the mitral valve closing click to the AV opening click, IRT refers the interval time from the AV closing click to the mitral valve opening click, and ET refers the time from the AV opening click to the AV closing click.

Aortic elastic properties were evaluated by 1 observer (S.Z.) who was blinded to the fetal biometry and cardiac information using vector velocity imaging software (VVI; Siemens Medical Solutions USA, Inc.). First, high-quality cine loop clips (38–56 frames/s) of the great artery short-axis view and LV outflow tract sagittal view were separately acquired in the absence of maternal breathing and analyzed offline. The tricuspid and pulmonary valve were required to be clearly visible in the great arteries short-axis view, and the mitral and aortic valves were required to be clearly shown in the sagittal view. The semilunar valves were used to guarantee a straight AA in cross or longitudinal sections, and atrioventricular valve motion was used to determine the cardiac cycle in the subsequent procedure. Second, aortic elastic properties such as the global circumferential strain (GCS) and fractional area change (FAC) were measured in short-axis view as previously reported.<sup>13,14</sup> In brief, a single still frame of the AA with optimal blood-intima border visualization was chosen for manual tracing. Then, aortic circumferential strain for systole and diastole were automatically calculated and displayed in a segment model. GCS was

calculated as the average of all 4 segmental systolic peak circumferential strains and recorded. In addition, the VVI technique provided the largest cross-sectional area (CSA) and smallest CSA of the traced AA in the short-axis view, and the FAC was calculated automatically as the percent change in the cross-sectional area:  $FAC (\%) = \frac{\text{largest CSA} - \text{smallest CSA}}{\text{largest CSA}} \times 100$  (Figure 1). Third, longitudinal strain of the AA was measured in the aorta sagittal view. Briefly, the anterior and posterior walls of the AA were traced separately beginning at the level of the sinotubular junction and ending at the level of the roof of the left atrium. Then, the longitudinal strain of the traced aortic wall was provided automatically (Figure 2). The mean longitudinal strain (MLS) of the AA was calculated as the mean systolic peak longitudinal strain in both the anterior and posterior walls. All aortic elastic property values (ie, the GCS, FAC, and MLS) were measured 3 times and averaged.

Data are presented as the median (range) or frequency (percentage). The Shapiro–Wilk W test was performed to assess the normality of the distribution. Data were compared between groups using Student *t*-test, the Mann–Whitney *U* test, the Chi-square test, or Fisher exact test as appropriate. The elastic properties of the aorta at the first and last examinations in utero were evaluated by a paired *t*-test. Spearman correlation coefficients were calculated to demonstrate the relationship between aortic elastic properties and cardiovascular biometrics in fetuses with CoA. Two-sided  $P < 0.05$  was considered significant. The intraclass correlation coefficient was used to assess the intraobserver and interobserver agreement on aortic elastic property parameters from 30 randomly selected observations. All statistical analyses were performed using STATA 15 (Stata Corp LLC, College Station, TX)

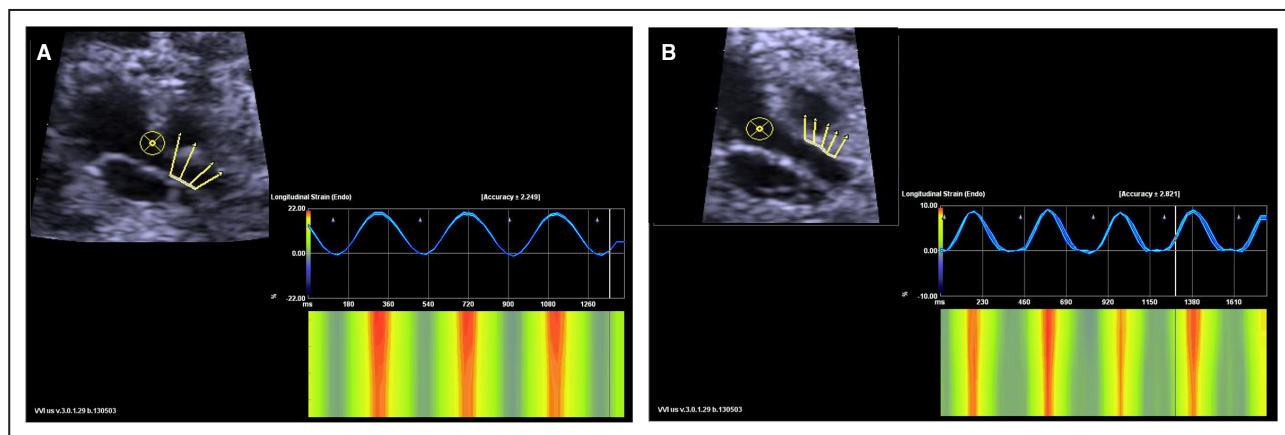


**Figure 2.** The mean longitudinal strain of the ascending aorta was obtained in a sagittal view by the velocity vector imaging technique.

The posterior (A) and anterior walls (B) of the ascending aorta were traced separately, and longitudinal strain was provided automatically. The mean longitudinal strain was calculated as the mean systolic peak longitudinal strain in both the anterior and posterior walls. VVI indicates velocity vector imaging.

and GraphPad Prism 4 (GraphPad Software, Inc., San Diego, CA).

## RESULTS

In total, 77 fetuses with suspected CoA were initially enrolled in this prospective study. Among them, 21 were excluded: 12 with no CoA on postnatal evaluation, 4 with terminated pregnancy, and 5 without follow-up. Finally, 56 fetuses with CoA and 56 GA-matched normal controls were enrolled. The first scan took place at a median GA of 29.3 (range, 22.3–35.4) weeks. The median follow-up period was 8 (range, 4–16) weeks. The clinical and cardiac information, rather than the aortic mechanics, of 18 fetuses in the CoA group were reported in our previous study.<sup>10</sup> The clinical characteristics of this cohort are summarized in Table 1. The echocardiogram dates of the cohort are summarized in Table 2. The aorta and mitral valve were smaller in CoA fetuses than in normal control fetuses at both the first and last scans ( $P<0.001$ ). The MPI-LV in the CoA group was larger than that of the normal group during the fetal period (the mean differences between CoA

and normal group were 0.04 [95% CI, 0.02–0.04] and 0.06 [95% CI, 0.03–0.08] for the first scan and second scans, respectively, both  $P<0.001$ ).

The GCS, FAC, and MLS in fetuses with CoA were significantly smaller than those in the normal control fetuses at both the first and last examinations in utero (18.50% versus 37.73% for GCS, 38.90% versus 57.55% for FAC, 6.61% versus 11.81% for MLS at first scan, 16.62% versus 42.05% for GCS, 36.54% versus 59.7% for FAC, 6.2% versus 11.46% for MLS at last scan, all  $P<0.001$ , Figure 3). There were no differences in the GCS, FAC, or MLS between the first and last scans both in the normal group and CoA group. The CoA group was further classified as the CoA fetuses with and without abnormal aortic valve morphology (ie, bicuspid and unicuspid aortic valve) based on the postnatal confirmation. There were no significant differences in GCS, MLS, and FAC between the 2 subgroup CoA fetuses ( $P>0.05$ , Figure S1).

There were negative correlations between aortic elastic properties (GCS, MLS, and FAC) and MPI-LV and positive correlations between aortic elastic properties and aortic isthmus size in fetuses with CoA ( $P<0.05$ , Figure 4).

**Table 1. Clinical Characteristics of the Cohort**

	CoA (n=56)	Control (n=56)	P value
<b>Maternal</b>			
Age, y	29 (20–42)	27 (22–38)	0.47
BMI, kg/m <sup>2</sup>	23 (18.4–28.6)	21.3 (18.3–27)	0.58
Nulliparous, n	36 (64%)	30 (53%)	0.34
<b>Fetal</b>			
GA at first scan, wks	29.3 (22.1–35.4)	29.3 (22.1–35.4)	1
EFW at first scan, g	1249 (418–2399)	1305 (444–2500)	0.18
GA at last scan, wks	38.3 (33.1–40.9)	37.3 (34.6–39.7)	0.17
EFW at last scan, g	2979 (2261–3618)	3100 (2188–3415)	0.29
<b>Delivery outcome</b>			
Vaginal delivery, n	43 (80.4%)	40 (83.9%)	0.67
GA at delivery, wks	39.6 (36.7–41.3)	39.4 (36.1–41)	0.12
<37 wks, n	2 (3.5%)	3 (5.3%)	1
Birth weight, g	2910 (2022–3602)	3218 (2941–3562)	<0.05
<10th centile	6 (10.7%)	0	<0.05
<b>Neonatal</b>			
5-min Apgar score <7, %	4 (7.1%)	0	0.12
Bicuspid aortic valve, n	24 (42.95)	0	<0.001
Unicuspid aortic valve, n	1 (1.8%)	0	1.0
Aortic stenosis, n	7 (12.5%)	0	<0.05
Hypoplastic aortic arch	8 (14.2%)	0	<0.01
Age at surgery, d	16 (5–59)	/	
NICU, %	7 (12.5%)	/	
Termo-terminal coarctectomy, n	17 (30.4%)	/	
Extended arch repair, n	39 (69.6%)	/	

Data are presented as the median (range) or frequency (percentage). BMI indicates body mass index; EFW, estimated fetal weight; GA, gestational age; and NICU, neonatal intensive care unit.

**Table 2. Fetal Echocardiogram and Aortic Elastic Properties of the Cohort**

	CoA (n=56)	Control (n=56)	P value
At first scan			
MV, z-score	-0.49 (-2.85 to 0.73)	0.20 (-1.51 to 1.44)	<0.001
TV, z-score	0.96 (-0.52 to 1.75)	-0.10 (-1.63 to 1.40)	<0.001
AV, z-score	-1.25 (-6.10 to -0.12)	0.07 (-1.50 to 1.30)	<0.001
AA, z-score	-1.54 (-5.73 to -0.26)	0.09 (-1.34 to 1.35)	<0.001
Isthmus in sagittal view, z-score	-4.11 (-6.05 to -2.55)	0.07 (-1.60 to 1.40)	<0.001
Isthmus in 3VT view, z-score	-3.82 (-5.68 to -2.36)	0.06 (-1.50 to 1.20)	<0.001
DAO, z-score	-0.43 (-1.07 to 0.42)	0.16 (-1.36 to 1.34)	<0.001
MPI-LV	0.45 (0.31 to 0.60)	0.31 (0.27 to 0.51)	<0.001
GCS, %	18.50 (10.40 to 40.78)	37.73 (20.88 to 81.39)	<0.001
FAC, %	38.90 (22.10 to 58.70)	57.55 (41.88 to 79.80)	<0.001
MLS, %	6.61 (1.90 to 13.17)	11.81 (6.29 to 18.25)	<0.001
At last scan			
MV, z-score	-0.61 (-3.04 to 0.67)	-0.10 (-1.52 to 1.40)	<0.001
TV, z-score	0.84 (-0.62 to 1.47)	0.03 (-1.40 to 1.20)	<0.001
AV, z-score	-1.35 (-6.20 to -0.39)	0.11 (-1.30 to 1.55)	<0.001
AA, z-score	-1.54 (-6.14 to -0.37)	-0.14 (-1.40 to 1.13)	<0.001
Isthmus in sagittal view, z-score	-4.51 (-6.30 to -2.55)	-0.27 (-1.44 to 1.20)	<0.001
Isthmus in 3VT view, z-score	-4.46 (-6.07 to -2.39)	-0.29 (-1.33 to 1.28)	<0.001
DAO, z-score	-0.60 (-1.52 to 0.90)	0.13 (-1.52 to 1.50)	<0.001
MPI-LV	0.45 (0.32 to 0.60)	0.39 (0.27 to 0.51)	<0.001
GCS, %	16.62 (10.21 to 36.91)	42.05 (16.87 to 67.39)	<0.001
FAC, %	36.54 (24.90 to 55.32)	59.70 (45.80 to 74.80)	<0.001
MLS, %	6.20 (2.28 to 16.56)	11.46 (5.36 to 23.49)	<0.001

Data are presented as the median (range) or frequency (percentage). 3VT indicates 3-vessel trachea views; AA, ascending aorta; AV, aortic valve; DAO, descending aorta; FAC, fractional area change; GCS, global circumferential strain; MLS, mean longitudinal strain; MPI-LV, modified left ventricular myocardial performance indexes; MV, mitral valve; and TV, tricuspid valve.

The intraclass correlation coefficients for the GCS, FAC, and MLS with the same observer were 0.91 (95% CI, 0.882–0.941), 0.93 (95% CI, 0.889–0.951), and 0.92 (95% CI, 0.853–0.956), respectively. The intraclass correlation coefficients for the GCS, FAC, and MLS between the 2 observers were 0.89 (95% CI, 0.807–0.943), 0.90 (95% CI, 0.832–0.937), and 0.91 (95% CI, 0.822–0.941), respectively.

## DISCUSSION

In this study, decreases in the FAC and circumferential and longitudinal strain of the AA were observed in the CoA group. To the best of our knowledge, this study is the first to indicate the impairment of aortic elastic properties in fetuses with CoA. Furthermore, such impaired aortic elastic properties are associated with diminished heart function and aortic isthmus size.

The MLS, GCS, and FAC of the fetal AA were diminished significantly in the CoA group compared with those in the normal control group, demonstrating reduced aortic wall deformation and aortic area change even in utero in fetuses with CoA. The MLS and GCS

derived from the speckle tracking technique VVI represent the stretch amount of the speckles along the aortic wall in the longitudinal and circumferential directions separately throughout the cardiac cycle, and the FAC reflects the extent of the change in the cross-sectional area of the aortic wall during the cardiac cycle. Previous experiments have reported significant negative associations between aortic mechanical parameters (strain and FAC) computed by VVI and the collagen content in aortic wall tissue<sup>17</sup> and elastin soluble fragment amount in plasma.<sup>18</sup> As an elastic reservoir, a healthy aorta expands in all directions in systole after absorbing part of the LV force and recoils during diastole to guarantee continuous blood flow to the periphery, depending on the normal wall structures and functional biomechanics. However, in CoA fetuses, structural abnormalities (cystic medial necrosis,<sup>19</sup> elastic fiber fragmentation<sup>7</sup>) in the ascending aortic wall could impair ascending aortic elasticity and consequently cause a reduction in ascending aortic deformation longitudinally and circumferentially.

This study evaluated the progress of aortic elastic properties in utero and found that there were

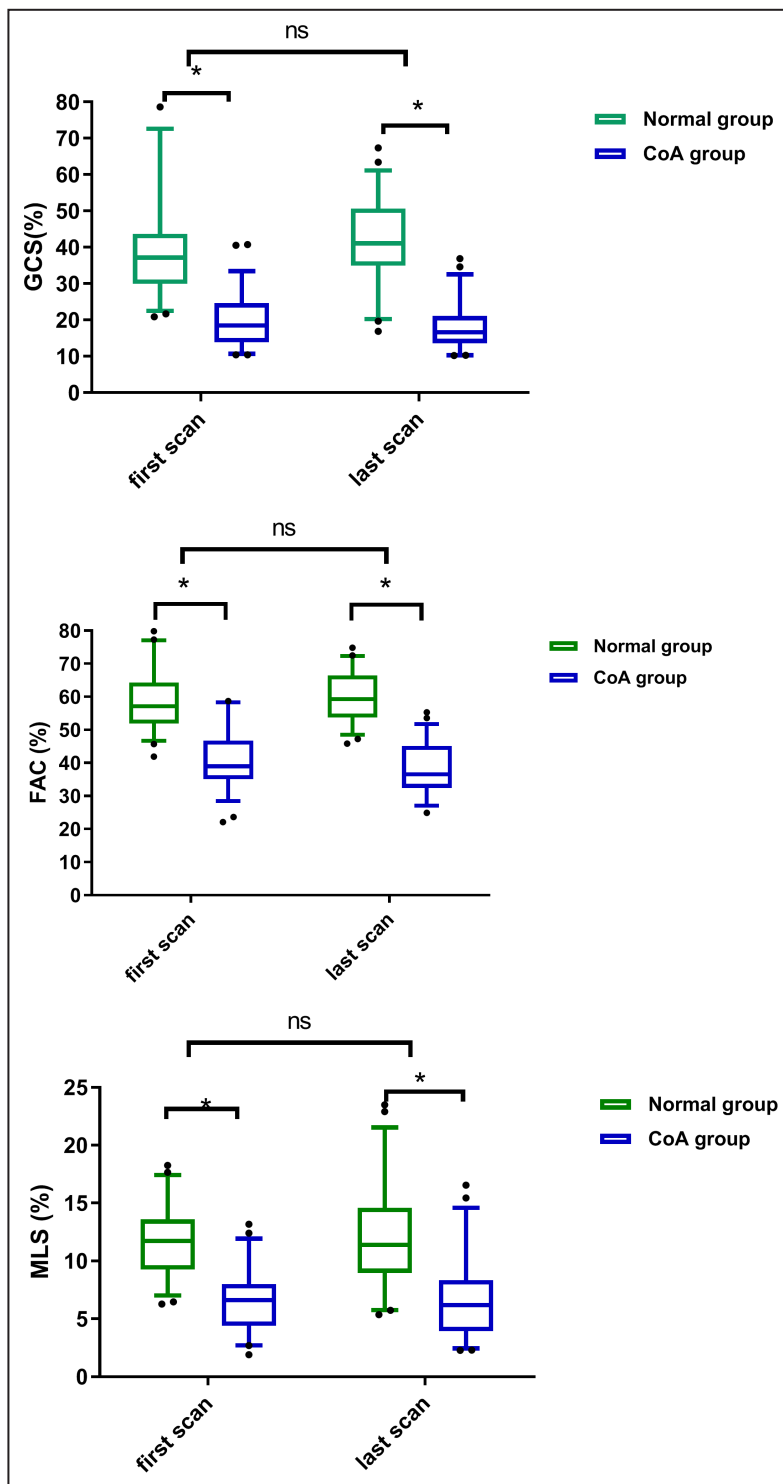


**Figure 3.** The global circumferential strain, fractional area change, and mean longitudinal strain decreased significantly in fetuses with coarctation of the aorta at both the first and last examination compared with those in the normal control group.

FAC indicates fractional area change; GCS, global circumferential strain; MLS, mean longitudinal strain; and ns, no significance. \* $P < 0.001$ .

apparently progressive declines in the GCS and FAC, but not the MLS, at the last examination in fetuses with CoA. Both the GCS and FAC were acquired from a

cross-sectional view of AA and enabled the assessment of entire vessel wall motion mechanics and lumen area changes of the traced region of AA. The MLS was

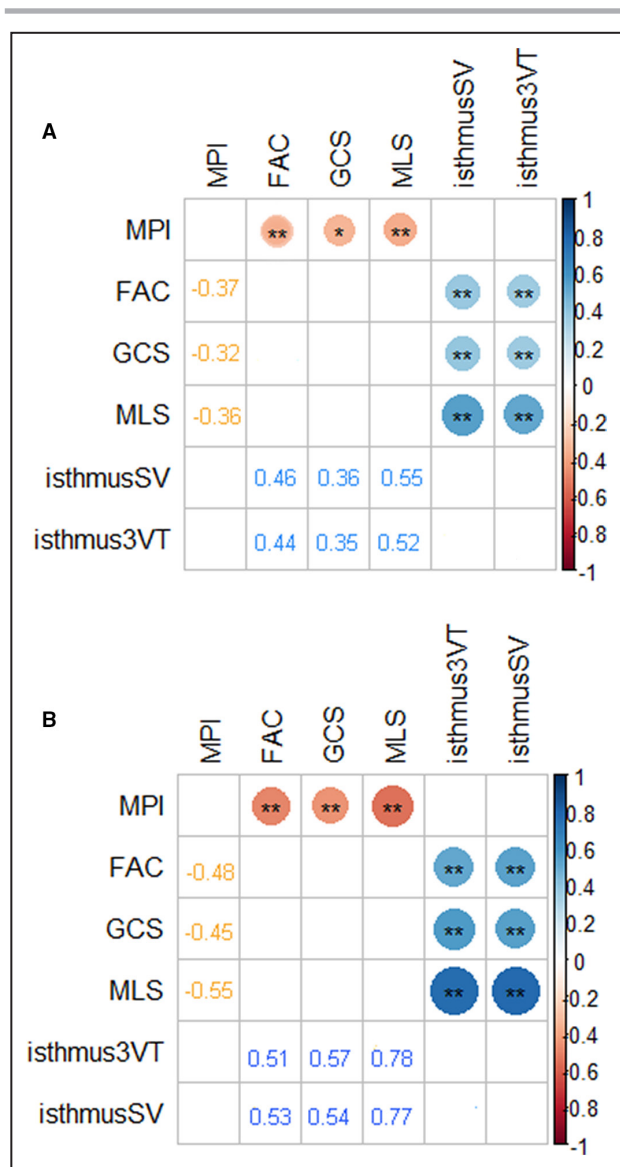


**Figure 4.** The correlation plot matrix between aortic elastic properties and isthmus size and left ventricular performance indexes at the first scan (A) and last scan (B). FAC indicates fractional area change; GCS, global circumferential strain; isthmus3VT, aortic isthmus z-score on 3-vessel trachea view; isthmusSV, aortic isthmus z-score in sagittal view; MLS, mean longitudinal strain; and MPI, myocardial performance index. \* $P < 0.05$ ; \*\* $P < 0.01$ .

acquired from the sagittal view of the AA, calculated as the mean longitudinal strain just from the anterior and posterior walls of the AA, and presented only part of the vessel wall mechanics. Therefore, technologically speaking, the GCS and FAC were supposed to be more comprehensive and more sensitive than the MLS for estimating impairment of the vessel wall mechanics.

This study showed inverse correlations between aortic elastic properties (GCS, MLS, and FAC) and MPI-LV in the CoA group, providing novel insight into ventricular–arterial coupling in utero. Altered

ventricular–arterial coupling has been described in patients with repaired CoA and is thought to promote hypertension.<sup>20</sup> Recently, our team<sup>21</sup> demonstrated the association of decreased ascending aortic diameter strain with impaired left E' and S' in the fetuses with CoA and first reported ventricular–arterial interactions in fetuses with CoA. Vessel distensibility is influenced by not only vessel elasticity but also cardiac contractility and cardiac output.<sup>22</sup> A previous study by our team and others observed decreased LV global strain, strain rate in systole and diastole,<sup>9</sup> ventricular FAC, transverse fractional shortening, and ejection fraction<sup>23</sup> in fetuses with CoA, which, together with the increased MPI-LV observed in this study, suggest depressed fetal heart contractility and diastolic function in CoA. On the one hand, impaired ventricular performance may cause decreased aortic stretching and thus a reduction in vascular wall deformation. In addition, neurohumoral and sympathetic activation triggered by stroke volume reduction deteriorates vascular dysfunction.<sup>24</sup> On the other hand, impaired ascending aortic elastic properties may augment LV afterload and thus myocardial oxygen demand, resulting in heart dysfunction.<sup>24</sup>

This study showed positive correlation between aortic elastic properties (GCS, MLS, and FAC) and aortic isthmus size in the CoA group, suggesting the potential role of isthmus narrowing in the development of impaired aortic elasticity. There is no doubt that the smaller the aortic isthmus size, the greater the pressure gradient and the afterload, which may generate abnormal wall shear stress in AA. Supraphysiological wall shear stress is recognized to be a mechanotransduction stimulus<sup>25</sup> that initiates injury to the endothelium, promotes the phenotypic change and apoptosis of smooth muscle cells, triggers oxidative stress and additional inflammation, mediates extracellular remodeling, and can eventually lead to impaired intrinsic properties of the aorta. Animal experiments<sup>26</sup> demonstrated that high-grade coarctation resulted in increased systolic blood pressure and plaque matrix content proximal to the coarctation compared with those in mild coarctation. Recently, Ylinen et al's population-based study<sup>27</sup> showed a negative association between preoperative aortic isthmus diameter and arm-leg blood pressure gradient and systolic blood pressure at follow-up in children with repaired CoA.

### Limitations

This study has several limitations. First, the frame rate in the VVI technique was still relatively low, especially compared with fetal heart rates of up to 120 to 160 bpm. Reasonable reduction in the scanning area and optimization of the focus position and depth were applied to increase the frame rate as much as possible. In this study, the medium frame rate was 45 (range, 38–56 frames/s),



which was similar to a previous study<sup>9-11</sup> evaluating fetal cardiac deformation by VVI and showed good performance on interobserver agreement. Second, there is a large subset of CoA fetuses (44.6%, 25/56) with abnormal aortic valve morphology. Bicuspid aortic valve has its own associated aortopathy that could potentially confound the analysis of CoA aortopathy, although we did not demonstrate differences of aortic elastic properties in this subset of CoA fetuses in this study. Third, the effect on cardiovascular morbidity of impaired elastic properties was not followed up. The exact predictive values of the GCS and FAC on the presence of aortopathy (ie, hypertension) or progressive ventricular–arterial coupling abnormalities in babies with CoA need further large-scale longitudinal study.

## CONCLUSIONS

Aortic strain and the fractional area change were decreased in fetuses with CoA. Impairment of these aortic elastic properties were correlated with diminished heart function in utero. Further large-scale longitudinal studies are required to confirm these findings and identify the predictive value on subsequent cardiovascular morbidity of such aortic wall elastic dysfunction in utero.

## ARTICLE INFORMATION

Received August 31, 2022; accepted December 7, 2022.

### Affiliations

Department of Ultrasound Diagnosis (R.X., D.Z., Y.L., M.Y., M.L., Q.Z., S.Z.); Department of Urology (R.X.) and Department of Cardiology and Cardiovascular surgery, The Second Xiangya Hospital, Central South University, Changsha, Hunan, China (L.X.).

### Sources of Funding

This study was supported by the State Natural Sciences Foundation of China (nos. 81501497 and 81871372) and Natural Science Foundation of Hunan Province (no. 2019JJ40425). The funding body was not involved in the design of the study; the collection, analysis, and interpretation of the data; or the writing of the manuscript.

### Disclosures

None.

### Supplemental Material

Figure S1

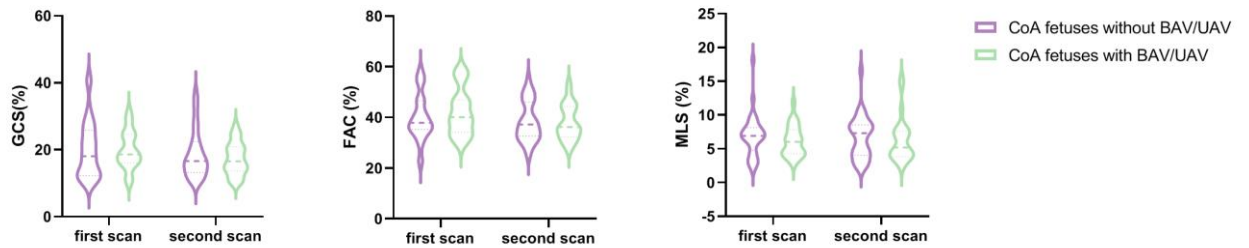
## REFERENCES

- Hoffman JI, Kaplan S. The incidence of congenital heart disease. *J Am Coll Cardiol*. 2002;39:1890–1900. doi: 10.1016/S0735-1097(02)01886-7
- Rosenthal E. Coarctation of the aorta from fetus to adult: curable condition or life long disease process. *Heart*. 2005;91:1495–1502. doi: 10.1136/hrt.2004.057182
- Kim YY, Andrade L, Cook SC. Aortic coarctation. *Cardiol Clin*. 2020;38:337–351. doi: 10.1016/j.ccl.2020.04.003
- Kowalski R, Lee MGY, Doyle LW, Cheong JLY, Smolich JJ, d'Udekem Y, Mynard JP, Cheung MMH. Reduced aortic distensibility is associated with higher aorto-carotid wave transmission and central aortic systolic pressure in young adults after coarctation repair. *J Am Heart Assoc*. 2019;8:e011411. doi: 10.1161/JAHA.118.011411
- Clarkson PM, Nicholson MR, Barratt-Boyes BG, Neutze JM, Whitlock RM. Results after repair of coarctation of the aorta beyond infancy: a 10 to 28years follow-up with particular reference to late systemic hypertension. *Am J Cardiol*. 1983;81:1541–1548. doi: 10.1016/0002-9149(83)90661-6
- Vogt M, Kühn A, Baumgartner D, Baumgartner C, Busch R, Kostolny M, Hess J. Impaired elastic properties of the ascending aorta in newborns before and early after successful coarctation repair: proof of a systemic vascular disease of the prestenotic arteries? *Circulation*. 2005;111:3269–3273. doi: 10.1161/CIRCULATIONAHA.104.529792
- Niwa K, Perloff JK, Bhuta SM, Laks H, Drinkwater DC, Child JS, Miner PD. Structural abnormalities of great arterial walls in congenital heart disease: light and electron microscopic analyses. *Circulation*. 2001;103:393–400. doi: 10.1161/01.CIR.103.3.393
- Peng QH, Zhou QC, Zeng S, Tian LQ, Zhang M, Tan Y, Pu DR. Evaluation of regional left ventricular longitudinal function in 151 normal fetuses using velocity vector imaging. *Prenat Diagn*. 2009;29:1149–1155. doi: 10.1002/pd.2386
- Zeng S, Zhou J, Peng Q, Deng W, Zang M, Wang T, Zhou Q. Sustained chronic maternal hyperoxygenation increases myocardial deformation in fetuses with a small aortic isthmus at risk for coarctation. *J Am Soc Echocardiogr*. 2017;30:992–1000. doi: 10.1016/j.echo.2017.05.008
- Xu R, Zhou J, Zhou Q, Zeng S. Decreased biventricular myocardial deformation in fetuses with lower urinary tract obstruction. *BMC Pregnancy Childbirth*. 2020;20:459. doi: 10.1186/s12884-020-03152-y
- Zeng S, Zhou Q, Zang M, Zhou J, Peng Q. Features and outcome of fetal cardiac aneurysms and diverticula: a single center experience in China. *Prenat Diagn*. 2016;36:68–73. doi: 10.1002/pd.4714
- Kim KH, Park JC, Yoon HJ, Yoon NS, Hong YJ, Park HW, Kim JH, Ahn Y, Jeong MH, Cho JG, et al. Usefulness of aortic strain analysis by velocity vector imaging as a new echocardiographic measure of arterial stiffness. *J Am Soc Echocardiogr*. 2009;22:1382–1388. doi: 10.1016/j.echo.2009.08.024
- An HS, Baek JS, Kim GB, Lee YA, Song MK, Kwon BS, Bae EJ, Noh CI. Impaired vascular function of the aorta in adolescents with turner syndrome. *Pediatr Cardiol*. 2017;38:20–26. doi: 10.1007/s00246-016-1478-4
- Petrini J, Jenner J, Rickenlund A, Eriksson P, Franco-Cereceda A, Caidahl K, Eriksson MJ. Elastic properties of the descending aorta in patients with a bicuspid or tricuspid aortic valve and aortic valvular disease. *J Am Soc Echocardiogr*. 2014;27:393–404. doi: 10.1016/j.echo.2013.12.013
- Schneider C, McCrindle BW, Carvalho JS, Hornberger LK, McCarthy KP, Daubeney PE. Development of Z-scores for fetal cardiac dimensions from echocardiography. *Ultrasound Obstet Gynecol*. 2005;26:599–605. doi: 10.1002/uog.2597
- Van Mieghem T, Gucciardo L, Lewi P, Lewi L, Van Schoubroeck D, Devlieger R, De Catte L, Verhaeghe J, Deprest J. Validation of the fetal myocardial performance index in the second and third trimesters of gestation. *Ultrasound Obstet Gynecol*. 2009;33:58–63. doi: 10.1002/uog.6238
- Kim SA, Lee KH, Won HY, Park S, Chung JH, Jang Y, Ha JW. Quantitative assessment of aortic elasticity with aging using velocity-vector imaging and its histologic correlation. *Arterioscler Thromb Vasc Biol*. 2013;33:1306–1312. doi: 10.1161/ATVBAHA.113.301312
- Longobardo L, Carerj ML, Pizzino G, Bitto A, Piccione MC, Zucco M, Oreto L, Todaro MC, Calabrò MP, Squadrito F, et al. Impairment of elastic properties of the aorta in bicuspid aortic valve: relationship between biomolecular and aortic strain patterns. *Eur Heart J Cardiovasc Imaging*. 2018;19:879–887. doi: 10.1093/ehjci/jex224
- Isner JM, Donaldson RF, Fulton D, Bhan I, Payne DD, Cleveland RJ. Cystic medial necrosis in coarctation of the aorta: a potential factor contributing to adverse consequences observed after percutaneous balloon angioplasty of coarctation sites. *Circulation*. 1987;75:689–695. doi: 10.1161/01.CIR.75.4.689
- Shang Q, Sarikouch S, Patel S, Schuster A, Steinmetz M, Ou P, Danford DA, Beerbaum P, Kutty S. Assessment of ventriculo-vascular properties in repaired coarctation using cardiac magnetic resonance-derived aortic, left atrial and left ventricular strain. *Eur Radiol*. 2017;27:167–177. doi: 10.1007/s00330-016-4373-8
- Zhou D, Xu R, Zhou J, Xie L, Xu G, Liu M, Zeng S. Aortic elasticity and cardiac function in fetuses with aortic coarctation. *Front Cardiovasc Med*. 2022;9:870683. doi: 10.3389/fcvm.2022.870683

22. Wohlmuth C, Moise KJ Jr, Papanna R, Gheorghe C, Johnson A, Morales Y, Gardiner HM. The influence of blood pressure on fetal aortic distensibility: an animal validation study. *Fetal Diagn Ther*. 2018;43:226–230. doi: [10.1159/000477396](https://doi.org/10.1159/000477396)
23. DeVore GR, Jone PN, Satou G, Sklansky M, Cuneo BF. Aortic coarctation: a comprehensive analysis of shape, size, and contractility of the fetal heart. *Fetal Diagn Ther*. 2020;47:429–439. doi: [10.1159/000500022](https://doi.org/10.1159/000500022)
24. Ikonomidis I, Aboyans V, Blacher J, Brodmann M, Brutsaert DL, Chirinos JA, De Carlo M, Delgado V, Lancellotti P, Lekakis J, et al. The role of ventricular-arterial coupling in cardiac disease and heart failure: assessment, clinical implications and therapeutic interventions. A consensus document of the European Society of Cardiology Working Group on Aorta & Peripheral Vascular Diseases, European Association of Cardiovascular Imaging, and Heart Failure Association. *Eur J Heart Fail*. 2019;21:402–424.
25. Staarmann B, Smith M, Prestigiacomo CJ. Shear stress and aneurysms: a review. *Neurosurg Focus*. 2019;47:E2. doi: [10.3171/2019.4.FOCUS19225](https://doi.org/10.3171/2019.4.FOCUS19225)
26. Baron BW, Glagov S, Giddens DP, Zarins CK. Effect of coarctation on matrix content of experimental aortic atherosclerosis: relation to location, plaque size and blood pressure. *Atherosclerosis*. 1993;102:37–49. doi: [10.1016/0021-9150\(93\)90082-6](https://doi.org/10.1016/0021-9150(93)90082-6)
27. Ylinen MK, Pihkala JI, Salminen JT, Sarkola T. Predictors of blood pressure and hypertension long-term after treatment of isolated coarctation of the aorta in children—a population-based study. *Interact Cardiovasc Thorac Surg*. 2022;35:ivac212. doi: [10.1093/icvts/ivac212](https://doi.org/10.1093/icvts/ivac212)

# **SUPPLEMENTAL MATERIAL**

**Figure S1. Violin plot of the aortic elastic properties between CoA fetuses with and without BAV/UAV.**



MLS, mean longitudinal strain; FAC, fractional area change; GCS, global circumferential strain; BAV, bicuspid aortic valve; UAV, unicuspid aortic valve.